Korean J. Chem. Eng., 37(12), 2334-2339 (2020)
DOI: 10.1007/s11814-020-0643-x

pISSN: 0256-1115
eISSN: 1975-7220

Investigation of fabrication methods for a cathode using a non-precious metal catalyst in polymer electrolyte membrane fuel cell

Bongho Lee, Jong Gyeong Kim, and Chanho Pak†

Graduate Program of Energy Technology, School of Integrated Technology, Institute of Integrated Technology, Gwangju Institute of Science and Technology, Gwangju 61005, Korea
(*Received 13 April 2020 • Revised 17 June 2020 • Accepted 19 July 2020*)

Abstract−As the need for fuel cell systems increases, much research is underway to replace platinum catalysts. Therefore, non-precious metal catalysts composed of inexpensive metal have attracted attention. Along with catalyst development, the importance of electrode development is emphasized. In this study, two manufacturing methods using a commercial non-Pt catalyst (FeNC) for cathode were adopted to investigate the effect of the method on the performance of membrane electrode assembly (MEA) for polymer electrolyte membrane fuel cell (PEMFC). Additionally, the effect of different ionomer ratios in the catalyst slurry compositions on the electrode was studied. As a result, the MEA with cathode fabricated by the spray method displayed 2.87-times higher performance than that of MEA with cathode by gas diffusion electrode that is manufactured using the Doctor-blade method. The higher performance of the spray electrode is attributed to the large portions of the pores under 10 nm in the electrode estimated by the mercury intrusion porosimetry. Therefore, it is important to generate large numbers of mesopores to fabricate a high-performance electrode of the non-precious metal catalyst for PEMFC.

Keywords: Non-precious Metal Catalyst, Fabrication Method, Spray Coating, Polymer Electrolyte Membrane Fuel Cell

INTRODUCTION

Environmental pollution problems, such as global warming, are increasingly being recognized and climate change conventions are being realized in the international community, recognizing the problem of carbon-based energy sources [1,2]. Due to the unstable supply of fossil fuel energy, which is mainly used in the world, researches on renewable energy to find alternative energy sources are being actively carried out, with many researchers paying attention to hydrogen energy [3,4]. Because hydrogen can be obtained from water, if water electrolysis technology is secured, it can obtain an unlimited energy source and is attracting attention as a future energy source because of its high energy density [3-8]. As a result, more attention has been focused on fuel cells that use hydrogen as a fuel [3,4,8]. In addition, commercial fuel cell electric vehicles have recently been in operation, and various applications utilizing hydrogen fuel cells such as ships and drones have been actively developed [8]. Depending on the various hydrogen-related technologies, the demand for catalysts is anticipated to surge further in the future [9]. Particularly, Pt catalysts have been mainly applied to fuel cells. Pt reserves are limited and concentrated in some regions, especially in South Africa [10]. As a result, there are concerns that there will be more problems in the future, such as higher Pt prices and reduced resources. Therefore, many researchers have been carrying out studies to increase the activity while lowering the amount of platinum to lower the price of the systems [11-14]. For this purpose, much research has been done on Pt-alloys, Pt de-alloys, core-shell catalyst, and non-precious metal catalysts (MPNC) for several decades [15-21]. Among them, the development of NPMC, especially FeNC-based catalysts with activity for oxygen reduction reaction (ORR) have been attracting great attention as an alternative to lower the cost of the catalysts because it does not use precious metal components.

Along with the development of FeNC-based catalysts, FeNC-based catalysts having ORR activity similar to that of Pt catalysts have been reported [14,25-27]. However, to realize performance in the membrane electrode assembly (MEA) level similar to that of the Pt catalyst, the catalyst layer must be at least four-times larger than that of the Pt catalyst [28,29]. Thus, it is still demanded the investigation of the fabrication method for cathode using the NPMC because the research on the electrode manufacturing has not progressed much.

In this study, the MEA performance of the commercial FeNC catalyst cathode manufactured by two different methods such as spray method and gas diffusion electrode (GDE) method was investigated. MEA performance was also measured according to the different ionomer content such as 37.5, 50, and 60 wt% in the catalyst ink. As a result, the MEA with cathode from the spray method (0.43 A/cm^2 at 0.6 V) showed improved performance compared with the MEA using cathode from the GDE method (0.15 A/cm^2 at 0.6 V). The enhancement of the MEA performance is accounted for the large portions of the mesopores around 10 nm of the electrode in the structural view, which is suggested by the mercury intrusion porosimetry. Additionally, this MEA performance difference by the fabrication method is attributed to the differences in the charge transfer resistance in the electrochemical aspect, which

†To whom correspondence should be addressed.
E-mail: chanho.pak@gist.ac.kr

is provided by the electrochemical impedance spectroscopy.

EXPERIMENTAL

1. MEA Fabrication

1-1. Spray Method

MEA fabrication was carried out in the order of catalyst ink dispersion, catalyst ink coating, catalyst layer drying, transfer, and cell assembling. Non-precious metal-based FeNC catalyst with 0.5% Fe (PMF-011904, Pajarito Power) and 20 wt% Pt/C (RTX) catalyst were used as catalysts for cathode and anode, respectively. The carbon that self-generated during the synthesis process of commercial FeNC was partially graphitized, which is comparable to Vulcan XC-72 carbon. The catalyst inks were prepared by first hydrating the catalyst in deionized water and then mixing catalyst with isopropanol (IPA) and the 20 wt% ionomer (EW-825, 3M) together. The ionomer content was set to the weight of the ionomer compared to the catalyst layer after drying. The ionomer content was based on 50 wt% in order to sufficiently cover the carbon, and 37.5 and 60 wt% were tested to find the optimal ratio by additionally adjusting the amount of ionomer [30-32]. Solvents for catalyst inks consisted of deionized water (DW) and IPA. The weight ratio of DW to IPA in the slurry was fixed to be 1 : 2 [9,30]. The solid content of the ink containing the catalyst was adjusted to be 3-4 wt% [33]. Thereafter, the catalyst inks were mixed using a magnetic stirrer for 1 h, and then the ink was dispersed for 30 min using Ultrasonic Processor (750 W). The catalyst ink was stirred for one day to stabilize the inks. After ink preparation, the inks were directly sprayed on a membrane (Nafion® 211) using a hand spray-gun (Gunpiece GP 1, Fuso Seiki Co.). During the spray, the membrane was fixed on the hot plate at 80 °C to remove solvents quickly. Catalyst coated membrane (CCM) was prepared by first spraying the anode and then spraying the cathode. CCM was then dried in a convection oven at 60 °C overnight. The active area of the electrode was 9 cm^2 (3×3 cm^2). Spray method MEA was fabricated by assembling CCM with the gas diffusion layer (GDL, JNTG A2-30). The loading of the FeNC catalyst on the cathode was 3 mg/cm^2 and the Pt loading on the anode was 0.1 mg/cm^2. The cell was cross-tightened with eight bolts using a torque wrench at 6 N m.

1-2. Gas Diffusion Electrode Method

MEA with gas diffusion electrode (GDE) method was fabricated using ball-milled catalyst ink. In the catalyst ink preparation, deionized water and a catalyst were initially added to a ball jar to hydrate the catalyst to prevent the firing, and dipropylene glycol (DPG) : DW was mixed at a ratio of 1 : 1 by weight, then the ionomers described above were added together. The solid content of all the catalyst inks was about 16-20 wt%. The catalyst ink was homogeneously mixed using ball milling for 1 h [34,35]. The prepared catalyst ink was coated on the cathode GDL at a rate of 10 mm/s using a doctor blade. Anode was prepared by directly coating on the membrane in the same way as the manufacturing method of 2.1.1. Coated GDE and anode were then dried in a convection oven at 60 °C overnight. GDE-method MEA was fabricated by assembling the above cathode and anode. There is a paper for the GDE method hot pressing reduces the performance of the electrode by decreasing the pores of FeNC electrode. Therefore, to prevent electrode performance reduction, MEA was prepared without hot pressing [36]. The loading of the FeNC catalyst on the cathode was 3 mg/cm^2 and the Pt loading on the anode was 0.1 mg/cm^2.

2. Electrochemical Analysis and Single-cell Test

The gasket for gas-sealing used was 235 and 290 μm for anode and cathode, respectively. Gasket, GDL, and electrode were tightened without the hot-pressing process by torque wrench at 6 N m. The thickness of the electrode was compressed to 80% of the pris-

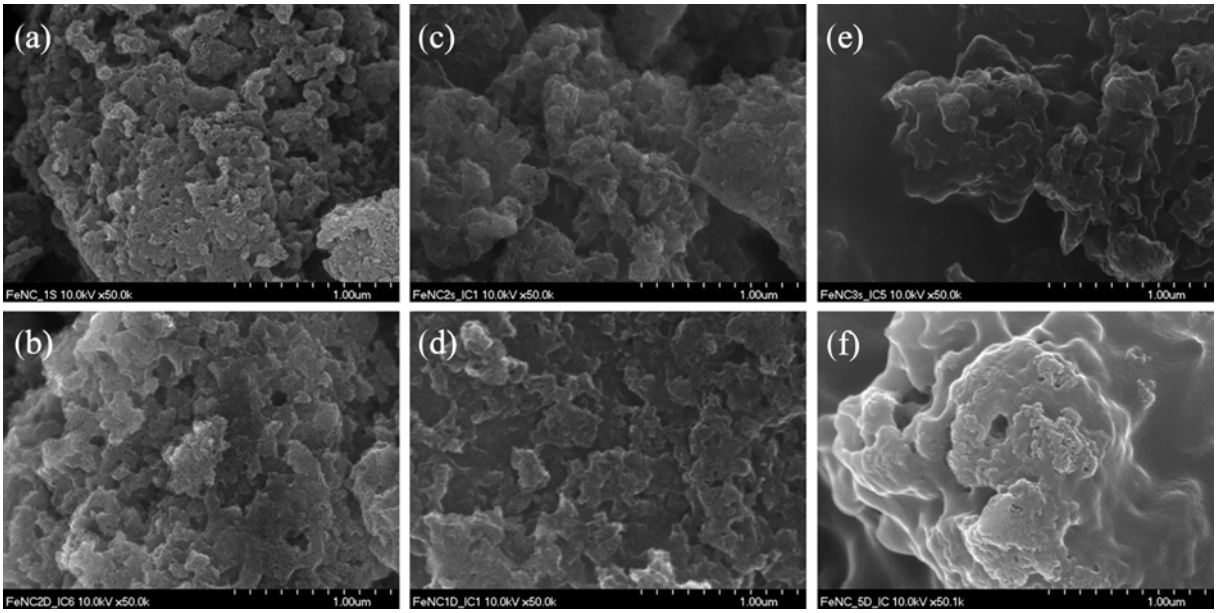

Fig. 1. SEM images of the cathode layer fabricated by spray method (a) ionomer content of 37.5 wt%, (c) ionomer content of 50 wt% and (e) ionomer content of 60 wt% and GDE method (b) ionomer content of 37.5 wt%, (d) ionomer content of 50 wt% and (f) ionomer content of 60 wt%.

tine thickness. After tightening, the single cell was hydrated by supplying hydrogen and nitrogen at a rate of 130 sccm at 65 °C with 100% relative humidity (RH), respectively. Cyclic voltammetry (CV) test was performed at 0.05-1.0 V before the cell test. After the CV test, the atmosphere of the MEA was changed by supplying hydrogen and oxygen, respectively at 65 °C at 100 kPa backpressure for the anode and 200 sccm for the cathode. I-V polarization curves were obtained using a fuel cell test station (Scitech Korea Co. Inc.) by increasing the current density of the single cell. Electrochemical impedance spectroscopy (EIS) was measured at 0.4, 0.6, and 0.8 V, respectively, for the MEA having sprayed cathode, over the frequency range from 10 kHz to 0.01 Hz [35,37]. However, EIS was measured at 0.6 V for the MEA having the cathode by GDE for comparison.

3. MEA Characterization

The surface morphology of MEAs was analyzed by the scanning electron microscope (SEM) (Hitachi S-4700 Field Emission SEM with an accelerating voltage of 10 kV). The pore size distribution of the electrodes was measured using mercury intrusion porosimetry (MIP) (Micromeritics Autopore V 9600).

RESULTS AND DISCUSSION

1. Physical Characterization

From SEM images (Fig. 1), there was no significant difference in electrode surface morphology according to the manufacturing method. As the ionomer content increased, it could be observed that the pores were blocked. At the ionomer content of 60 wt%, many pores were covered with ionomers. On the other hand, when the ionomer content was 37.5 wt%, many pores were observed. The surface of the electrode is considered to be affected by the ratio of the ionomer more than the electrode manufacturing method. It is reported that the pore distribution of the electrode affects the performance of the electrode. In Fig. 2, the electrode from the spray method displays a larger portion of the mesopore between 30-100 nm than those of the electrode prepared by the GDE method regardless of ionomer content. Well-developed mesopores can improve oxygen transport by reducing the O_2 diffusion distance, resulting in enhanced performance of MEA with sprayed-cathode than that of MEA with cathode by bar-coating [38-41]. The more pores smaller than 10 nm when forming the electrode, the performance was improved [42]. As a result of analyzing the pore distribution of the electrode formed by two different methods in this experiment, it was observed that about 10 nm of pores were mainly distributed in the electrode manufactured by the spray method. On the other hand, the electrode manufactured by the blade coating did not have many pores of less than 10 nm. It is considered that the main reason for the difference in MEA performance between the blade method and the spray method is due to small pores of about 10 nm. It has been considered that as more mesopores develop, the more ORR active -N and -Fe sites could be easily exposed to oxygen molecules, which contributes to the improvement of MEA performance [40,43,44]. Besides, mesopores have an additional effect on exposing the active site [43]. Comparing the electrodes with different fabrication methods, more pores around 10 nm developed in the spray electrode than the GDE electrode. Therefore, the spray method is considered to less reduce the number of active sites in the catalyst distributed in small pores rather than the GDE method.

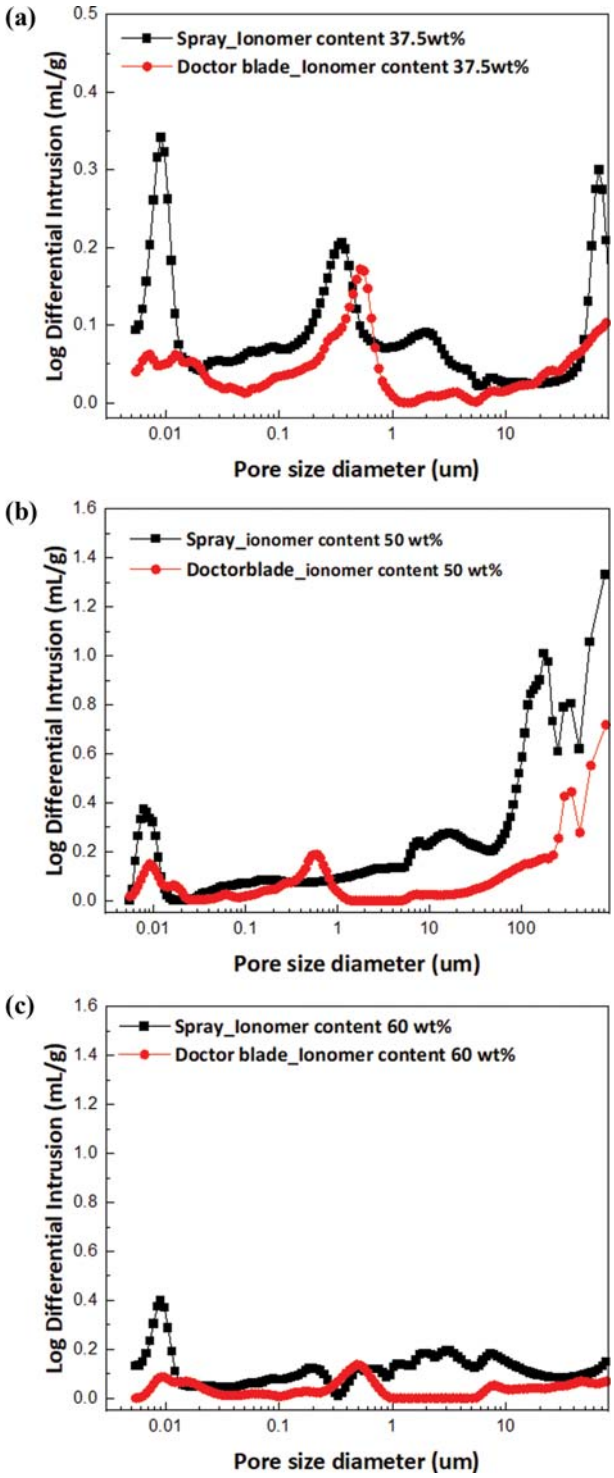

Fig. 2. The pore size distribution estimated from the mercury intrusion porosimetry from the electrode having difference ionomer content.

2. MEA Performance

Fig. 3 shows the I-V polarization curves according to the elec-

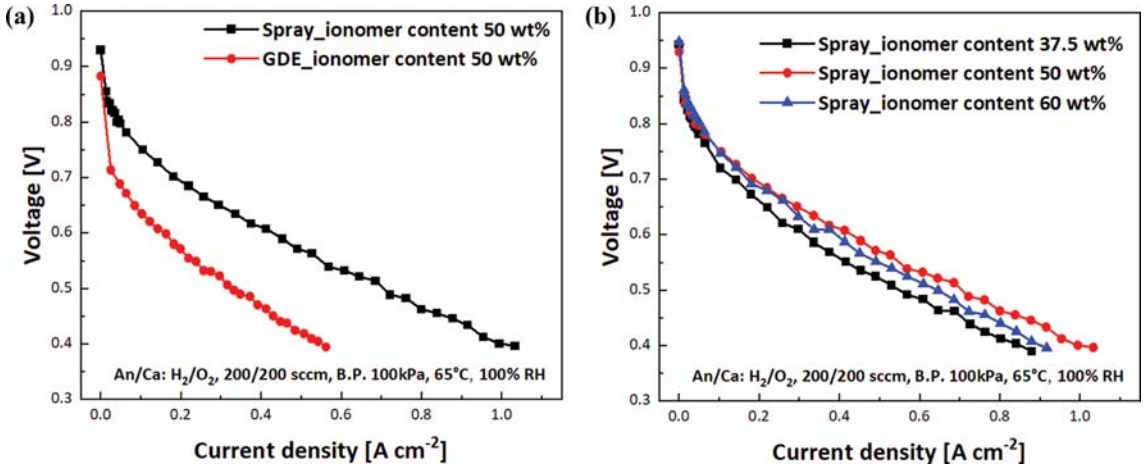

Fig. 3. (a) MEA performance for comparing the electrode from spray and GDE methods, (b) change of the MEA performance by the ionomer contents.

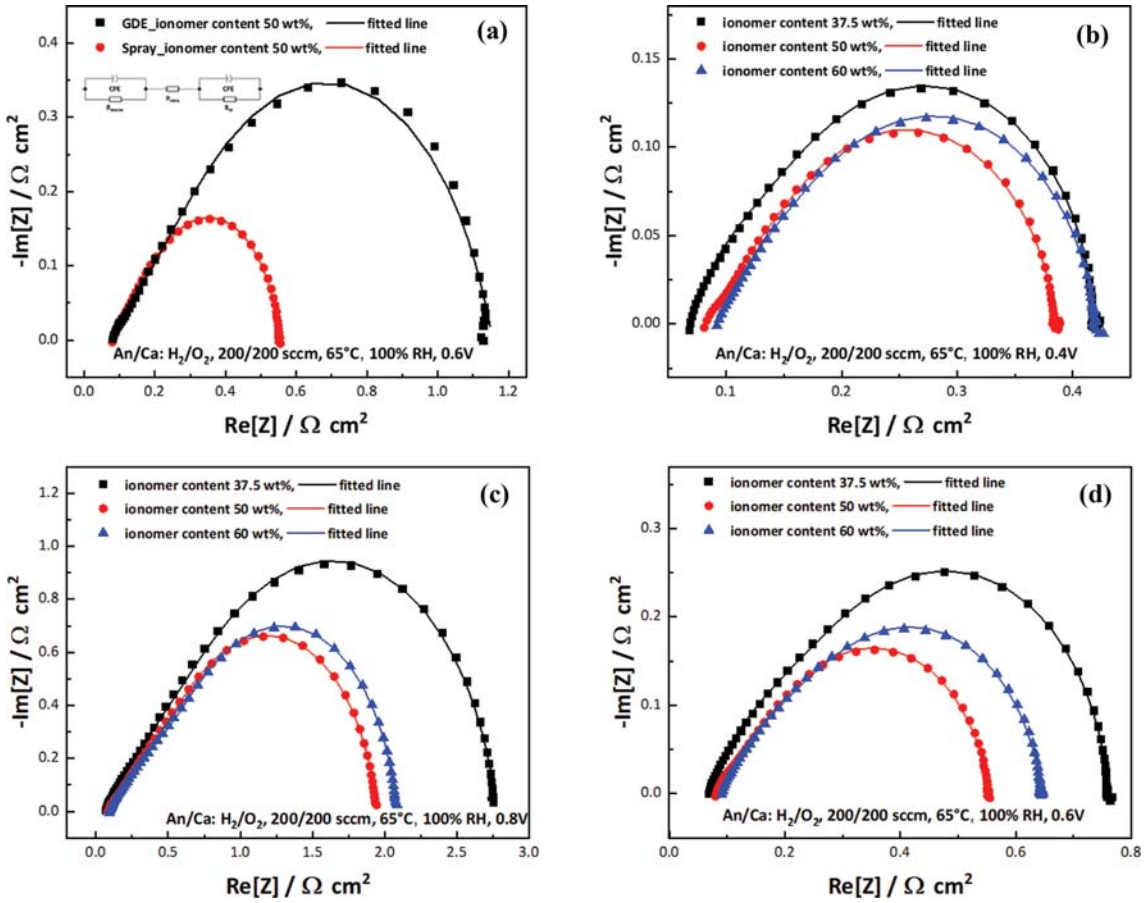

Fig. 4. Nyquist plots from electrochemical impedance spectroscopy. (a) MEAs with sprayed cathode and GDE cathode at 0.6 V, (b) MEAs by sprayed cathode with ionomer content at 0.4 V, (c) MEAs by sprayed cathode with ionomer content at 0.6 V, and (d) MEAs by sprayed cathode with ionomer content at 0.8 V.

trode manufacturing method and ionomer content. In Fig. 3(a), the electrode fabricated by the spray method (0.43 A/cm^2 at 0.6 V) is 2.87-times greater than the GDE method (0.15 A/cm^2 at 0.6 V). The main reason for the difference in MEA performance between spray and GDE methods is the presence of 10 nm mesopores. Three cathodes with varying ionomer content were prepared to find the proportion of ionomers that properly cover the catalyst. Comparing the MEA performance according to ionomer content in the spray method, the current density was 0.31, 0.43, and 0.39 A/cm^2 at 0.6 V according to the ionomer content of 37.5, 50, and 60 wt%,

Table 1. EIS analysis of spray and GDE method MEAs

Voltage (V)	Method	Ionomer contents (wt%)	R_{Ω} ($\Omega \cdot cm^2$)	$R_{Ct,A}$ ($\Omega \cdot cm^2$)	$R_{Ct,C}$ ($\Omega \cdot cm^2$)
0.4 V	Spray	37.5	0.07031	0.09741	0.2513
	Spray	50	0.08451	0.08091	0.2204
	Spray	60	0.09417	0.08562	0.2402
0.6 V	Spray	37.5	0.06997	0.2428	0.4479
	Spray	50	0.08140	0.1919	0.2884
	Spray	60	0.09197	0.1908	0.3628
	GDE	50	0.07829	0.2464	0.8297
0.8 V	Spray	37.5	0.07411	0.7962	1.9098
	Spray	50	0.08796	0.6725	1.1919
	Spray	60	0.09606	0.7471	1.2483

respectively. The electrode with ionomer content of 37.5 wt% has lower MEA performance than that of the electrode with ionomer content of 50 wt% because the insufficient amount of ionomers in the electrode does not cover the catalyst sufficiently [30]. When the ionomer content increases from 37.5 to 60 wt%, it can be observed that the utilization of the catalyst increases and the MEA performance of the electrode in the kinetic region improves. However, the electrode with high ionomer content (60 wt%) is difficult to remove water, resulting in a decrease of the MEA performance compared to the 50 wt% in mass transfer regions [28,36].

3. Electrochemical Analysis

EIS data according to the manufacturing method and ionomer content after fuel cell testing are displayed in Fig. 4. Table 1 lists the fitting values of EIS data using the equivalent circuit in inset of Fig. 4(a). From the EIS data, charge transfer resistance of anode ($R_{ct,A}$) and the cathode ($R_{ct,C}$) and bulk resistance (R_{Ω}) were extracted using an equivalent circuit as shown in Fig. 4(a) [35,45]. The $R_{ct,C}$ (0.2884 $\Omega \cdot cm^2$) of the electrode by the spray method is 3.3-times smaller than the $R_{ct,C}$ (0.8297 $\Omega \cdot cm^2$) by the GDE method at 0.6 V as listed in Table 1. Comparing the resistance components of the two electrodes, $R_{ct,C}$ show the largest difference between the three components. The EIS analysis suggests that the difference in MEA performance is related to the $R_{ct,C}$ differences. In the EIS analysis of the electrodes with various ionomer content, the electrode with ionomer content of 37.5 wt% displayed higher resistance than the other two electrodes in both $R_{ct,A}$ and $R_{ct,C}$, which is attributed to the inadequate distribution of ionomer on the catalyst, resulting in lower catalyst utilization. At 0.4 and 0.6 V, the overall trends did not change. However, it was confirmed that the R_{ct} difference between MEA having 37.5 wt% and 50 wt% ionomer content reduced with decreasing voltage, and the R_{ct} difference between MEA with 60 wt% and 50 wt% ionomer decreased with increasing voltage. Through these results, it could be inferred that at the low voltage region, MEA performance is improved with a low ionomer content. Conversely, high ionomer content is advantageous in high voltage regions. The electrode with the ionomer content of 60 wt% had a 10% difference in MEA performance from the electrode with the ionomer content of 50 wt%. From CV measurements as shwon in Fig. 5, the oxygen reduction peaks were observed as 0.724 V (50 wt%), 0.713 V (60 wt%), 0.692 V (37.5 wt%), respectively. Oxygen reduction peaks showed a similar trend to the MEA performance results [39].

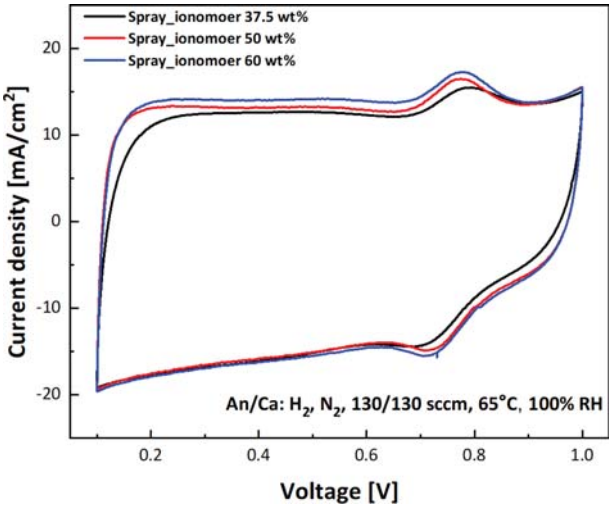

Fig. 5. CV measurements for MEAs from spray method at 65 °C.

CONCLUSIONS

An electrode was fabricated by the blade method and the spray method to find a suitable electrode manufacturing method for FeNC. The biggest difference in MEAs manufactured in two ways was due to the difference in porosity. The 10 nm mesopores were considered to have caused the MEA performance difference between the two electrodes. The difference in pores is attributed to the difference in drying time according to the electrode manufacturing method. Therefore, when manufacturing FeNC electrodes, it is important to have a way to shorten the electrode drying time in the electrode manufacturing process, such as the spray method.

ACKNOWLEDGEMENT

This research was supported by the National Research Founda-

tion of Korea (NRF-2018M1A2A2063174). C. Pak is also thankful for the support from the GIST Research Institute (GRI) grant (GK12490) funded by the GIST in 2020.

REFERENCES

1. C. J. Smith, P. M. Forster, M. Allen, J. Fuglestvedt, R. J. Millar, J. Rogelj and K. Zickfeld, *Nat. Commun.*, **10**, 101 (2019).
2. L. Velautham, M. A. Ranney and Q. S. Brow, *Front. Commnun.*, **4**, 7 (2019).
3. J. O. Abe, A. P. I. Popoola, E. Ajenifuja and O. M. Popoola, *Int. J. Hydrogen Energy*, **44**, 15072 (2019).
4. D. Parraa, L. Valverde, F. J. Pino and M. K. Patel, *Renew. Sust. Energy Rev.*, **101**, 279 (2019).
5. M. Carmo, D. K. Fritz, J. Mergel and D. Stolten, *Int. J. Hydrogen Energy*, **38**, 4901 (2013).
6. X. Bai, *Ambio*, **45**, 819 (2016).
7. D. Karapinar, N.-H. Tran, D. Giaume, N. Rankbar, F. Jaouen, V. Mougel and M. Fontecave, *Sust. Energy Fuels*, **3**, 1833 (2019).
8. A. Khaligh and Z. Li, *IEEE Transac. Vehicular Tech.*, **59**, 2806 (2010).
9. T. Reshetenko, A. Serov, K. Artyushkova, I. Matanovic, S. Stariha and P. Atanassov, *J. Power Sources*, **324**, 556 (2016).
10. W. Bernhart, S. Riederle, M. Yoon and W. G. Aulbur, *Auto Tech. Rev.*, **3**, 18 (2014).
11. H. A. Gasteiger, S. K. Shyam, B. Sompalli and F. T. Wagner, *Appl. Catal. B: Environ.*, **56**, 9 (2005).
12. J. Yang, S. Yang, Y. Chung and Y. Kwon, *Korean J. Chem. Eng.*, **37**, 176 (2020).
13. T. T. K. Huynh, T. Q. N. Tran, H. H. Yoon, W.-J. Kim and I. T. Kim, *Korean J. Chem. Eng.*, **36**, 1193 (2019).
14. S. T. Thompson and D. Papageorgopoulos, *Nat. Catal.*, **2**, 558 (2019).
15. D. D. Papadias, R. K. Ahluwalia, N. Kariukil, D. Myers, K. L. More, D. A. Cullen, B. T. Sneed, K. C. Neyerlin, R. Mukundan and R. R. L. Borup, *J. Electrochem. Soc.*, **165**, F3166 (2018).
16. S. Chen, P. J. Ferreira, W. Sheng, N. Yabuuchi, L. F. Allard and Y. Shao-Horn, *J. Am. Chem. Soc.*, **130**, 13818 (2008).
17. V. R. Stamenkovic, B. Fowler, B. S. Mun, G. Wang, P. N. Ross, C. A. Lucas and N. M. Marković, *Science*, **315**, 493 (2017).
18. H.-Y. Park, J. H. Park, P. Kim and S. J. Yoo, *Appl. Catal. B: Environ.*, **225**, 854 (2018).
19. R. Bashyam and P. Zelenay, *Nature*, **433**, 63 (2006).
20. H. Park, K. M. Kim, H. Kim, D.-K. Kim, Y. S. Won and S.-K. Kim, *Korean J. Chem. Eng.*, **35**, 1547 (2018).
21. A. K. Choudhary and H. Pramanik, *Korean J. Chem. Eng.*, **36**, 1688 (2019).
22. G. Wu and P. Zelenay, *Acc. Chem. Res.*, **46**, 1878 (2013).
23. J. H. Kim, Y. J. Sa, H. Y. Jeong and S. H. Joo, *ACS Appl. Mater. Interfaces*, **9**, 9567 (2017).
24. Y. J. Sa, D.-J. Seo, J. Woo, J. T. Lim, J. Y. Cheon, S. Y. Yang, K. M. Lee, D. Kang, T. J. Shin, H. S. Shin, H. Y. Jeong, C. S. Kim, M. G. Kim, T.-Y. Kim and S. H. Joo, *J. Am. Chem. Soc.*, **138**, 15046 (2016).
25. T. Asset and P. Atanassov, *Joule*, **4**, 33 (2020).
26. L. Osmieri, *Chemengineering*, **3**, 16 (2019).
27. Y.-Z. Wang, W.-Y. Huang, T.-H. Hsich, L.-C. Jheng, K.-S. Ho, S.-W. Huang and L. Chao, *Polymers*, **11**, 1368 (2019).
28. H. T. Chung, D. A. Cullen, D. Higgins, B. T. Sneed, E. F. Holby, K. L. More and P. Zelenay, *Science*, **357**, 479 (2017).
29. Y. Zhan, H. Zeng, F. Xie, H. Zhang, W. Zhang, Y. Jin, Y. Zhang, J. Chen and H. Meng, *J. Power Sources*, **431**, 31 (2019).
30. H. M. Barkholtz, L. Chong, Z. B. Kaiser, T. Xu and D.-J. Liu, *Int. J. Hydrogen Energy*, **41**, 22598 (2016).
31. Y. Li, X. Liu, L. Zheng, J. Shang, X. Wan, R. Hu, X. Guo, S. Hong and J. Shui, *J. Mater. Chem. A*, **7**, 26147 (2019)
32. S. K. Babu, H. T. Chung, P. Zelenay and S. Litster, *ECS Trans.*, **69**, 23 (2015)
33. M. J. Workman, M. Dzara, C. Ngo, S. Pylypenko, A. Serov, S. McKinney, J. Gordong, P. Atanassov and K. Artyushkova, *J. Power Sources*, **348**, 30 (2017).
34. E. You, M. Min, S.-A. Jin, T. Kim and C. Pak, *J. Electrochem. Soc.*, **165**, F3094 (2018).
35. M. Zhiani, S. Majidi, V. B. Silva and H. Gharibi, *Energy*, **97**, 560 (2016).
36. X. Yin, L. Lin, H.-T. Chung, S. K. Babu, U. Martinez, G. M. Purdy and P. Zelenay, *ECS Trans.*, **77**, 1273 (2017).
37. E. Lee, D.-H. Kim and C. Pak, *Appl. Surf. Sci.*, **510**, 145461 (2020).
38. H. Yu, L. Bonville and R. Maric, *J. Electrochem. Soc.*, **165**, J3318 (2018).
39. Y. Li, T. Liu, W. Yang, Z. Zhu, Y. Zhai, W. Gu and C. Zhu, *Nanoscale*, **11**, 19506 (2019).
40. Y. He, S. Liu, C. Priest, Q. Shi and G. Wu, *Chem. Soc. Rev.*, **49**, 3484 (2020).
41. Y.-Z. Wang, W.-Y. Huang, T.-H. Hsieh, L.-C. Jheng, K.-S. Ho, S.-W. Huang and L. Chao, *Polymers*, **11**, 1368 (2019).
42. X. Peng, T. Omasta, W. Rigdon and W. E. Mustain, *J. Electrochem. Soc.*, **163**, E407 (2016).
43. L. Xiao, Q. Yang, M. J. Wang, Z. X. Mao, J. Li and Z. Wei, *J. Mater. Sci.*, **53**, 15246 (2018).
44. G. A. Ferrero, K. Preuss, A. B. Fuertes, M. Sevilla and M.-M. Titirici, *J. Mater. Chem. A*, **4**, 2581 (2016).
45. A. M. Dhirde, N. V. Dale, H. Salehfar, M. D. Mann and T.-H. Han, *IEEE Trans. Energy Convers.*, **25**, 778 (2010).